MICROFLUIDIC FLOW CYTOMETER FOR HIGH THROUGHPUT LABEL FREE CELL ANALYSIS

by

SAJAL CHIRVI

Presented to the Faculty of the Graduate School of

The University of Texas at Arlington in Partial Fulfillment

of the Requirements

for the Degree of

MASTER OF SCIENCE IN BIOMEDICAL ENGINEERING

THE UNIVERSITY OF TEXAS AT ARLINGTON

AUGUST 2008

ACKNOWLEDGEMENTS

I would like to take this opportunity to express my sincere gratitude to all those people who have helped me throughout my thesis work.

This thesis could not have been written without Dr. Digant P. Davè who not only served as my supervisor but also encouraged and challenged me throughout my academic program. It is because of him that I got an opportunity to work on such an exciting project. Also, I would like to thank him for his assistance in the preparation of this thesis.

I would also like to thank Dr. Young Tae Kim, for giving me valuable inputs and feedback during our meetings, which eventually helped me refine my work.

My special thanks are also due to Dr. Cheng Jen Chuong, Professor, Dept. of Bioengineering, UTA and Dr. Robert Bachoo, Department of Neurology, UTSW for their prompt and valuable inputs.

I would also like to thank UTA for giving me such a challenging, supportive and technical environment. I owe you a lot.

I would like to thank my lab mate Sukanya Varadharajan for her constant technical support and help.

Finally, I am greatly indebted to my parents, Mrs. Teja Chirvi and Mr. Ashok Kumar Chirvi and my brother Jewel Chirvi, whose prayers and well wishes made this work possible. For me they are an institution of love and inspiration.

JULY 15, 2008

ABSTRACT

MICROFLUIDIC FLOW CYTOMETER FOR HIGH THROUGHPUT LABEL FREE CELL ANALYSIS

Sajal Chirvi, M.S.
The University of Texas at Arlington, 2008

Supervising Professor: Dr. Digant P. Davè

Microfluidic flow cytometer for high throughput label free cell analysis is proposed. Detection of cell morphology plays an important role in determination of state of health and diagnosis of many diseases such as sickle cell anemia, cancer, urine analysis, blood analysis etc. The platform proposed integrates label free cell analysis, microfluidic platform and high throughput imaging. Label free analysis helps in analyzing cells without altering cell/protein of interest and also allows biophysical characterization of living cells. Microfluidic platform used is fabricated from soft lithography. It mimics biological environment due to its channel confinement and is biocompatible. Being optically clear (PDMS), it is an excellent platform to image cells. High throughput cell imaging is achieved with phase contrast interferometer which can generate a phase map of important morphology parameters. Practically a throughput

20,000 cells/sec can be achieved using this setup. Optical setup with microfluidic platform can be integrated with surface enhanced Raman spectroscopy (SERS) for molecular detection. Although, setup proposed is suitable for any cell analysis application, it is ideal for circulating tumor cell which are just handful in a sample. High sensitivity of optical setup allows efficient detection of low population cells in a given sample.

TABLE OF CONTENTS

ACKNOWLEDGEMENTS iii

ABSTRACT iv

LIST OF ILLUSTRATIONS ix

LIST OF TABLES xii

CHAPTER Page

1. INTRODUCTION 1

1.1 Background and Significance 1

1.2 Need of High Throughput Cell Analysis 4

1.3 Current Techniques for Cell Analysis 4

1.3.1 Conventional Microscopic Examinations 4

1.3.2 Automatic Measurement Using Flat Sheath Flow 4

1.3.3 Flow Cytometer 5

1.4 Need of Label Free Imaging 6

1.5 Microfluidic Platform 7

1.6 Specific Aims 9

1.7 Organization of Thesis 9

2. DEVICE FABRICATION 11

2.1 Mask Design 12

2.2 Master Mold Fabrications 14

2.3 Casting PDMS Mold 19
2.4 Connecting Ports to Microfluidic Device 21
3. MICROFLUIDIC FLOW SETUP 23
3.1 Flow System Setup 23
3.2 Components of Flow Setup 24
3.2.1 Small Volume Delivery System 25
3.2.2 Microfluidic Device 26
3.2.3 Peristaltic Pump 31
3.2.4 Labjack 31
3.3 LABVIEW Module for Video and Image Acquision 32
4. OPTICAL SETUP FOR IMAGING 33
4.1 Differential Phase Contrast Interferometer (DPCI) 34
5. RESULTS 37
5.1 Characterization of microfluidic devices 38
5.2 PDMS modified surface hydophilicity test 39
5.3 Microscopic images of flowing sample 39
5.2.1 Images from device 1 39
5.2.2 Images from device 2 41
5.2.3 Images from device 3 44
5.4 Images obtained from DPCI setup 46
6. DISCUSSION AND CONCLUSIONS 47

7. FUTURE GOALS 49

APPENDIX

A. SOFTWARE INTERFACE 50

REFERENCES 52

BIOGRAPHICAL INFORMATION 54

LIST OF ILLUSTRATIONS

Figure Page

1: Microscopic view of different cells present in urine (a) White blood cell and red blood cells (b) squamous epithelial cells (c) red cell cast (d) white blood cells and bacteria..... 2

2: Block diagram representing different components of flow cytometer. 8

3: The processes involved in fabrication of master mold and microfluidic devices. Blocks in yellow indicate the use of clean room whereas rest of the blocks indicates processes accomplished outside clean room facility..... 12

4: Mask design for a basic one layer microfluidic device. It shows two reservoirs connected by a single channel..... 13

5: Mask design for a two layer microfluidic device.
(a) First layer showing two reservoirs connected by a single channel.
(b) Second layer showing just two reservoirs. 13

6: Mask design for a two layer microfluidic device.
(a) First layer showing two reservoirs connected by a multiple channels.
(b) Second layer showing just two reservoirs. 14

7: Flowchart showing the steps for fabrication of the master mold. These steps are carried out in clean room facility..... 15

8: Photograph of a master mold showing the microfluidic device. 19

9: Flowchart showing the steps for fabrication of the PDMS devices from master mold..... 20

10: Peeling of the cured PDMS devices from the master mold. 21

11: Global view of the microfluidic device with the input and output ports connected. 22

12: Block Diagram of the flow setup used for flowing sample

through the microfluidic device. 24

13: Small volume delivery system setup 25

14: Microfluidic device design 1. (a) Global view of the device
with input and output ports connected (b) zoomed in channel. 27

15: Microfluidic device design 2. (a) Global view of the device
with input and output ports connected (b) zoomed in channel. 28

16: Microfluidic device design 3. (a) Global view of the device
with input and output ports connected (b) zoomed in multiple channels. 29

17: Microfluidic device integrated on the microscope with input
and output ports connected. 30

18: Peristaltic pump used to create negative pressure in the microfluidic
device for allowing suction of fluid. 31

19: Front panel of LABVIEW VI for acquiring images of flowing beads,
cells and fluorescein. 32

20: Prototype (DPCI) system constructed using polarization
maintaining (PM) fiber. 34

21: Sample path configuration for recording brightfield and *en face* DPCI 35

22: Fluorescein in device # 1. a) fluorescein in input reservoir
b) & c) fluorescein in channel d) fluorescein in output reservoir. 40

23: Fluorescent beads in device # 1 a) beads in reservoir b) beads in channel 41

24: Epithelial cells in device # 1 a) cells in channel b) cells in reservoir. 41

25: Fluorescein in device # 2 a) fluorescein in input reservoir
b) & c) fluorescein in channel d) fluorescein in output reservoir. 42

26: Beads in device # 2 a) beads in channel (next to reservoir)
b) & c) beads stuck at interface between reservoir and channel
d) fluorescein in channel. 43

27: Epithelial cells in device # 2 a) cells in channel b) cells in reservoir. 44

28: Fluorescein in device # 3 a) fluorescein in input reservoir

b) & c) fluorescein in channels d) fluorescein in output reservoir. 45

29: Beads in device # 3 a) & b) beads lined up and stuck
in channel (next to reservoir) 45

30: DPCI (a & b) and bright field microscope images (c & d)
of single human epithelial cheek cells. Lateral (a) and collinear
(b) probe beam configuation were used to record DPCI images.
Color bar denotes optical path length in nanometers. 46

LIST OF TABLES

Table Page

1: The final ramp speed needed to get a desired thickness for a particular photoresist type. 16

2: Two step bake temperature for desired thickness and type of photoresist. 16

3: Exposure time needed for desired thickness and the type of photo-resist. 17

4: Two step post exposure bake temperatures for desired thickness and type of photoresist. 18

5: Development time needed for desired thickness and type of photo-resist. 18

6: Characterization of microfluidic device. 38

CHAPTER 1

INTRODUCTION

1.1 Background and Significance

The ability to image single cells in a platform by using a technique which is sensitive enough to detect morphological changes has vast clinical applications. Typically information about behavior, status, and health of the cells is collectively derived from activity of thousands or millions of them. A more precise understanding of differences between individual cells could lead to better treatments for cancer and diabetes. The imaging technique proposed can be used for blood analysis, urine analysis and cancer detection. It can also be used as a cell counter and at the same time cell morphology profiling can be achieved.

The analysis of body fluids is a vital part of diagnostic investigation of many patients. Approximately 60% of the entire adult human body is fluid. One-third of that fluid is found in the space outside the cell and includes blood, cerebral spinal fluid, saliva and urine. Abnormal body fluids provide a readily accessible source of diagnostic information. The clinician uses the information provided by body fluid analysis to formulate, in order of priority, a list of differential diagnoses and to follow the results of therapy [1, 2]. In the laboratory, it is a complex procedure, with multiple departments coordinating and generating reports on one patient's sample.

Although the platform proposed can be used for vast applications, urine cytology and detection of circulating tumor cells could be potential applications. Apart from clinical application this platform can also be used for research applications such as for studying red blood cell dynamics or cell adhesion assays.

The body's entire volume of blood plasma passes through the kidney and is filtered more than 60 times every day. Urine is nothing but a filtered blood, whatever body has in excess and is trying to regulate will appear in the urine. Urinalysis screens for a variety of disorders. The tests check color, odor, and cloudiness. They also detect and measure a variety of cells and substances in the urine. Abnormal findings indicate certain problems [3].

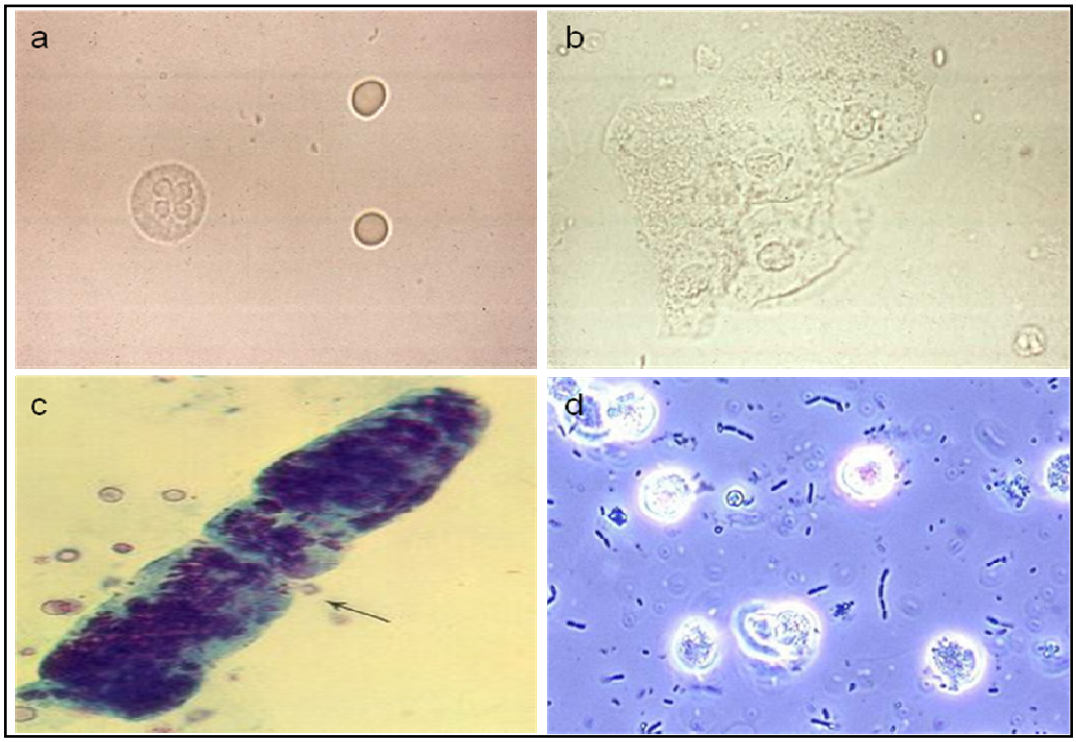

Figure 1: Microscopic view of different cells present in urine (a) White blood cell and red blood cells (b) squamous epithelial cells (c) red cell cast (d) white blood cells and bacteria.

Protein in the urine suggests kidney disease. Sugar usually indicates diabetes. Certain substances indicate liver disease. A variety of problems cause bleeding in the urinary tract. White blood cells indicate an infection in the urinary tract. Bacteria or yeast also indicate infection. Some types of kidney disease can cause plugs of material, casts; to form in tiny tubes in the kidneys. The casts then get flushed out in the urine. Casts can be made of red or white blood cells, waxy or fatty substances, or protein. The type of cast in the urine can help show what type of kidney disease may be present [4]. Figure 1 shows the microscopic views of some of these cells. Some abnormal findings are not caused by only one disease. Combined with other symptoms and history, they help doctors pinpoint diseases. They also provide an early warning for certain diseases.

Cells in the bodily fluids carry the most direct and complete information for screening and staging of cancer. Proteins and genes are also potential tumor biomarkers if present in detectable quantities. Though rarely is a single protein or gene tumor biomarker sufficient to reliably screen for cancer. Exfoliated tumor cells are indicative of cancer in the organ from which the fluid was expelled or extracted. Circulating tumor cells (CTC) in blood are indicative of cancer metastasis. CTC from metastasized lung, prostate, breast and colon cancer can be found in peripheral blood. The task of detecting tumor cells in bodily fluids with clinically acceptable results is difficult. For low levels of tumor cells it is akin to finding a needle in a haystack. Not only the presence of tumor cells has to be detected but they have to be counted with a high degree of accuracy. This is particularly true in the case of CTCs where there can be literally just a handful among millions of cells in the sample.

1.2 Need of High Throughput Cell Analysis

The analysis of the behaviour of individual cells is a field that is currently generating a wealth of new insights, especially in the fields of proteomics and analytical biotechnology. These systems offer a versatile environment in which low numbers of cells and molecules can be manipulated, captured and analysed. High-content single-cell analysis platforms can give meaningful insights into intrinsically heterogeneous cell populations. In particular, preclinical anti-cancer drug screening, phenotypic characterization of different parameters at a single cell level can be developed.

1.3 Current Techniques for Cell Analysis

1.3.1 Conventional Microscopic Examinations

One of the technique available in market for urine cell analysis include visual inspection of cells based on microscopy In this technique a sample of well-mixed urine is centrifuged until a moderately cohesive pellet is produced at the bottom of the tube. The supernate is decanted and sediment is re-suspended. A drop of re-suspended sediment is poured onto a glass slide, coverslipped and then examined under a microscope. The cells are observed, classified and counted under the microscope. However, this technique is labor intensive and suffers from lack of reproducibility[5, 6].

1.3.2 Automatic Measurement Using Flat Sheath Flow

The technique of automatic measurement using a combination of flat sheath flow and image processing technology, involves a video rate camera to capture an image of a urine specimen. The specimen is made to flow as a flat stream and images are taken which are then processed to identify the cells in the sample. This technique is costly as it

relies on image processing tools and its processing speed is low. The automation of device merely displays the images upon roughly classifying the imaged components based upon their size, and it is required that classification process be performed by a technician while the display is observed. Also, since the amount of urine specimen measured according to above techniques is very small, a drawback is that casts the discovery of the presence of which is very important cannot be discovered in the urine sediment [5].

1.3.3 Flow Cytometer

The flow cytometer measures the physical and chemical characteristics of cells. It can measure a cell's diameter, volume, surface area, and granularity based on forward and side light scattering. It identifies and quantifies different types of cells by their surface proteins. It determines a cell's internal structure, including its DNA content, enzymes, and proteins. The basic components of a flow cytometry are a source of light (laser), flow cell, optical components to focus light of different colors on to the detectors, electronics to amplify and process the resulting signals and a computer. Flow cytometric analysis involves measurements being made separately on each particle within the suspension in, and thus is a very important feature of flow cytometry [7, 8]. This setup interrogates just one cell at a time by taking advantage of hydrodynamic focusing in which sample is injected in middle of flow and two fluids sheath this sample and enables one cell to pass through point of interrogation. But the setup proposed here will interrogate a sheet of cells flowing through a channel thus elimination need of

hydrodynamic focusing. The setup will offer advantages of imaging more cells per unit time and will also relieve device from any pressure issues.

The major disadvantage of the conventional flow cytometry is that it can't efficiently indicate the ploidy state of individual cell. Also, when pairs of cells go by too close together to distinguish, they must both be discarded. There are losses in the yield. Running the high-speed sorter all day gets expensive, and may pose problems in keeping the cells in best condition during such a long sort. Finally there is the cost, which is hundreds of dollars per high-speed sort [9, 10].

1.4 Need of Label Free Imaging

Labels have enabled many scientific advances that would not otherwise have been possible. However, labels do have drawbacks. They disrupt the accurate measurements by altering the cell/protein of interest. Many of the currently available methods for detection require signal amplification or enrichment of the expression of fluorescent protein markers and antibodies in the cells. As a consequence, these methods tend to include additional steps and time-consuming assay procedures. A simple detection system that can achieve high sensitivity without the need for target amplification and labeling is highly desirable. Also fluorescence-based detection systems face issues, such as photo bleaching and quenching which are absent in label free detection techniques. Label-free methods also promise to offer better sensitivity, selectivity, and low cost for the detection [11]. We can study molecular interactions without modifying molecules of interest. Moreover the assays are cheaper and hazard free with less lab safety and waste

disposal issues/costs. A simple, inexpensive, and completely label-free method for detection of cells is presented [12].

1.5 Microfluidic Platform

Microfluidic device offers many advantages and it provides a powerful platform for biological Assays. Microfluidic systems provide an attractive and versatile platform for the manipulation, isolation and transport of selected cells. It is now possible to achieve quantitative, reliable data with these devices which compares favourably to standards attained from traditional cell culture methods and in vivo studies, making it a genuine alternative for high throughput cellular analysis. In microfluidics, small volumes of solvent, sample, and reagents are moved through microchannels embedded in a chip. Miniaturized versions of bioassays offer many advantages, including small requirements for solvents, reagents, and cells which are critical for valuable samples and for high-throughput screening, portability, low cost, versatility in design, and for integration with other miniaturized devices.

As the material of choice for microfluidic systems, polymers such as PDMS exhibit advantages over silicon and glass, because they are easy to fabricate, and compatible with the requirements of many bioassays . PDMS-based microfluidic systems can be used as a useful step to test new designs, or as a final product. The field lies at the interfaces between engineering, chemistry, and biology; and aims to develop lab-on-a-chip systems. Highly integrated micro devices show great promise for basic biomedical and pharmaceutical research, and robust and portable point-of-care devices could be used in clinical settings [13].

Hence, there is a need for a technique which has advantages over manual scoring, quantitative rather than qualitative scoring, ease of reproducibility, detection of more subtle changes than is possible by eye, and elimination of tedious manual labor and much faster analysis [14].

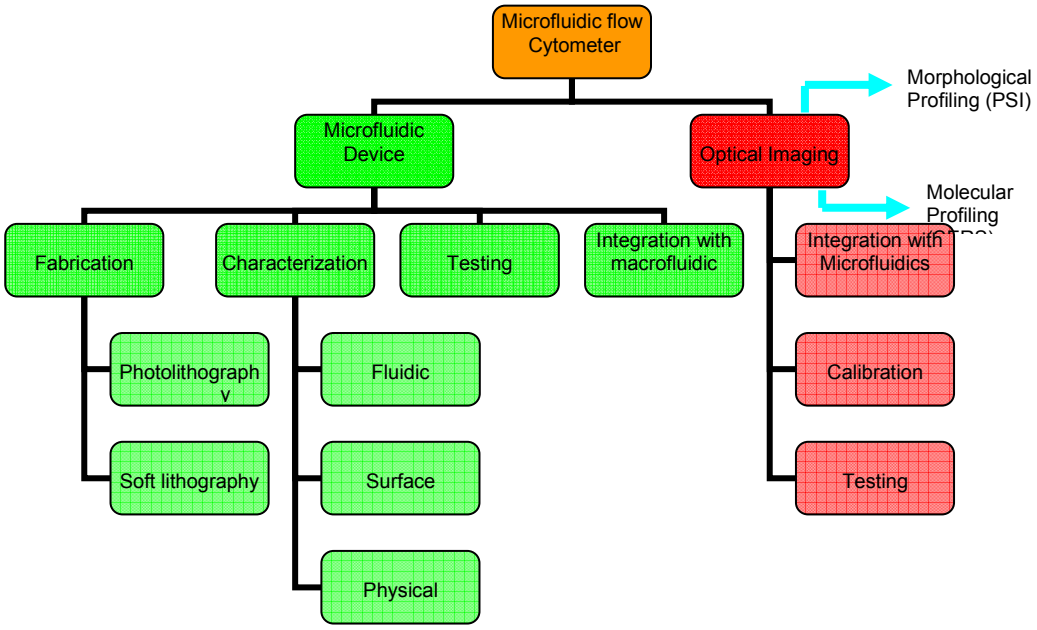

Figure 2: Block diagram representing different components of flow cytometer.

The microfluidic platform proposed for high throughput label free cell analysis is cost effective due to its less manufacturing cost and can analyze samples in clinician's office. Hence, a multitasking platform for cell morphology detection is presented. Figure 2 shows the block diagram of the flow cytometer device proposed. It shows the integration of microfluidic and optical setup.

1.6 Specific Aims

The primary objective of this thesis is to develop portable microfluidic platform which can be assembled on the microscope and the optics lined up for imaging a sheath of flowing label free cells.

The specific aims of this project are

1. Designing and fabricating a microfluidic device and optimizing them for cell flow.
2. Calibrating microfluidic flow cytometer by flowing fluorescein, fluorescent beads and cells.
3. Quantitatively imaging flowing cells using Differential Phase Contrast Interferometer (DPCI).

1.7 Organization of Thesis

This section describes the integration of label free detection of cells in microfluidic platform. It also lists the specific goals for this thesis.

Chapter 2 describes the designing and fabrication of microfluidic devices using a technique of soft lithography. This chapter if further divided in three sub parts. First part describes the fabrication of the master mold. Part two describes the procedure for making PDMS dies. Part three describes the port connection to the PDMS dies.

Chapter 3 describes the flow setup part of the flow cytometer through the microfluidic device. This section elaborates on individual component of flow system. Chapter concludes with discussion on software interfaces for controlling speed of peristaltic pump and video and image acquisition using LABVIEW module

Chapter 4 describes the basic imaging setup for Differental Phase Contrast Interferometer (DPCI). It also discusses the image acquisition through this setup.

Chapter 5 describes the results obtained from characterization of microfluidic devices as well as from PDMS surface hydrophilic characterization. It also discusses results obtained from flowing fluorescein, beads and epithelial cells. Results obtained from DPCI setup are also shown.

Chapter 6 briefs discussion and conclusions drawn from this project.

Chapter 7 summarizes the future work that will be integrated to the present setup.

CHAPTER 2

DEVICE FABRICATION

Soft lithography typically refers to the molding of a two-part polymer (elastomer and curing agent), called polydimethylsiloxane (PDMS), using photoresist masters. A PDMS device has design features that are only limited by the master from which it is molded [15]. It is faster, less expensive, and more suitable for most biological applications than glass or silicon micromachining. It provides a convenient, effective, and low-cost method for the formation and manufacturing of microstructures. In this technique, an elastomeric stamp such as polydimethylsiloxane (PDMS) with patterned relief structures on its surface is used to generate patterns and structures [16].

The steps involved in the photolithographic process are wafer cleaning; photoresist application; soft baking; mask alignment; exposure and development; and hard-baking. Figure 3 shows the steps involved in fabrication process of master mold and microfluidic devices. The blocks in yellow indicate the use of nanofab facility and yellow room facilty. The use of yellow room is mandatory because in white light, wafer coated with resist will get exposed.

SU-8 is a high contrast, epoxy based photoresist designed for micromachining and other microelectronic applications, where a thick chemically and thermally stable image is desired. The exposed and subsequently cross-linked portions of the film are rendered insoluble to liquid developers. SU- 8 has very high optical transparency above 360nm,

which makes it ideally suited for imaging near vertical sidewalls in very thick films. SU-8 is best suited for permanent applications where it is imaged, cured and left in place. This photoresist can be deposited at thicknesses up to 200 μm depending on the formulation of SU-8. The SU-8 comes in different viscosities for targeting different thicknesses. It can be used to pattern features with very high aspect ratios. Also, it adheres strongly to silicon substrate making it possible to increase the yield of PDMS dies [17].

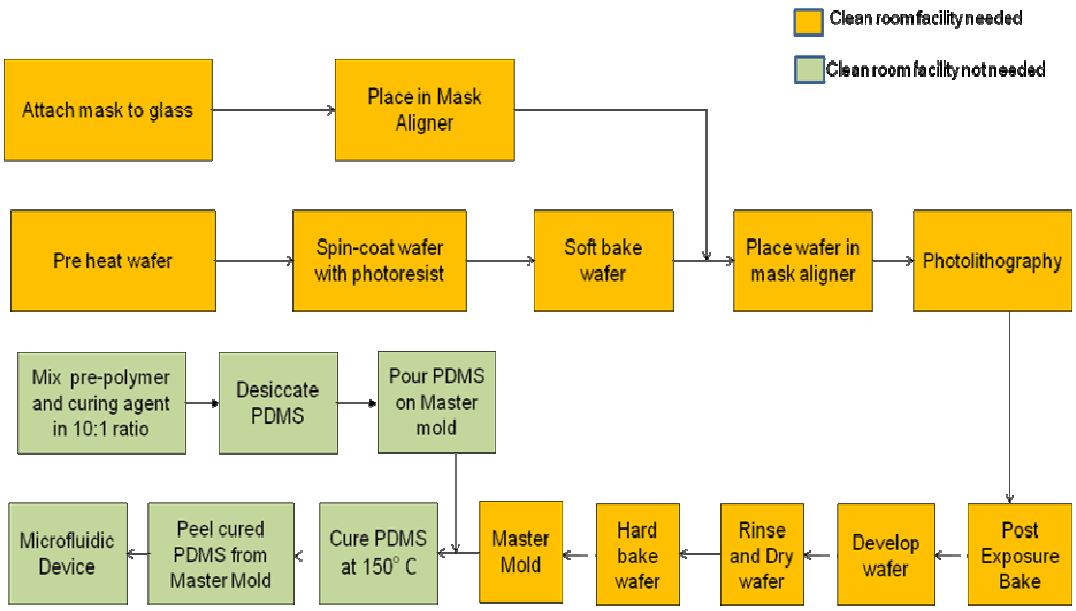

Figure 3: The processes involved in fabrication of master mold and microfluidic devices. Blocks in yellow indicate the use of clean room whereas rest of the blocks indicates processes accomplished outside clean room facility.

2.1 Mask Design

The device designs are made using the A9 CAD software. These designs are printed by a company using a laser printer on a mylar mask. The smallest feature size that can be reproduced on mask is 10 microns which is resolution of printer. Figure 4 shows the mask design of single layer flow cytometer device. This mask will produce a device

of constant depth throughout reservoirs and channel. Figure 5 and 6 shows the mask design of two layer flow cytometer device. Mask 5a and 6a shows the first layer and mask 5b and 6b shows the second layer for the microfluidic two layer devices.

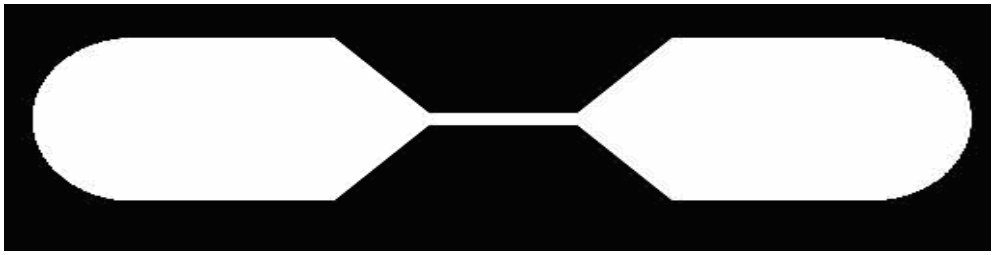

Figure 4: Mask design for a basic one layer microfluidic device. It shows two reservoirs connected by a single channel.

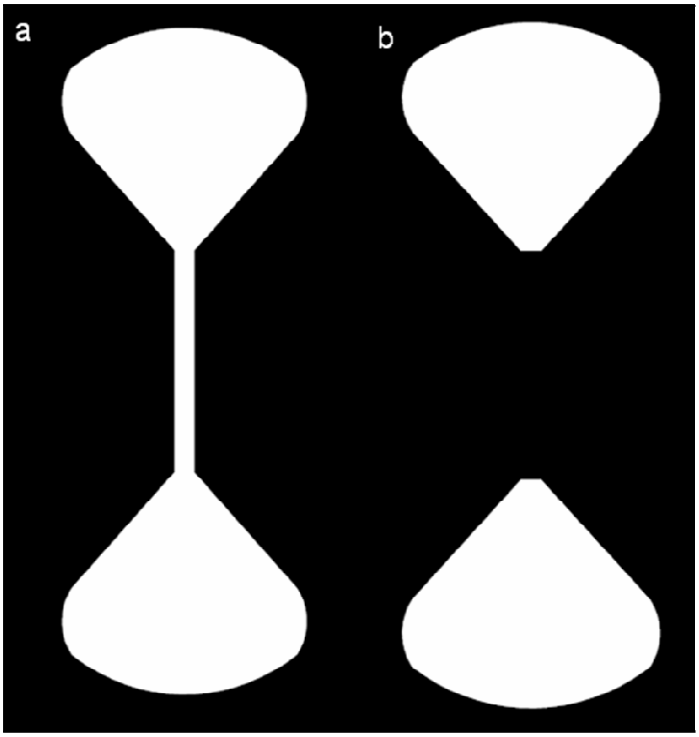

Figure 5: Mask design for a two layer microfluidic device. (a) First layer showing two reservoirs connected by a single channel. (b) Second layer showing just two reservoirs.

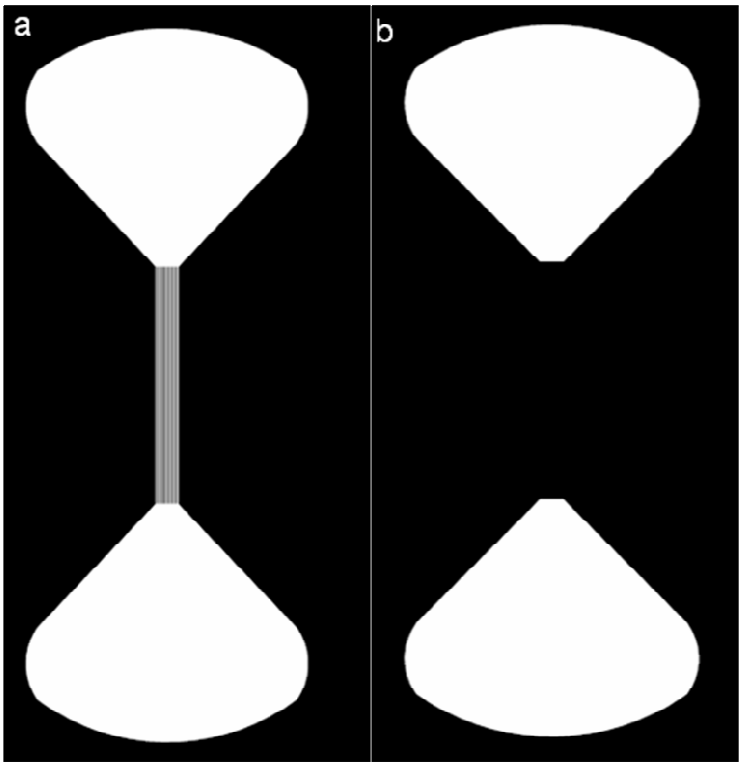

Figure 6: Mask design for a two layer microfluidic device. (a) First layer showing two reservoirs connected by a multiple channels. (b) Second layer showing just two reservoirs.

2.2 Master Mold Fabrications

A series of processes are done before having a master mold in hand. The flow chart in figure 7 shows the processes carried out for master mold fabrication. Initially the wafer is treated in corona discharge asher for about 5 minutes. It is done to get rid of any organic impurities on the silicon wafer. Then the wafer is dehydrated at 150° for about 10 minutes. These two steps ensure that the wafer is completely dehydrated and clean so that photo resist will have a better contact affinity for wafer.

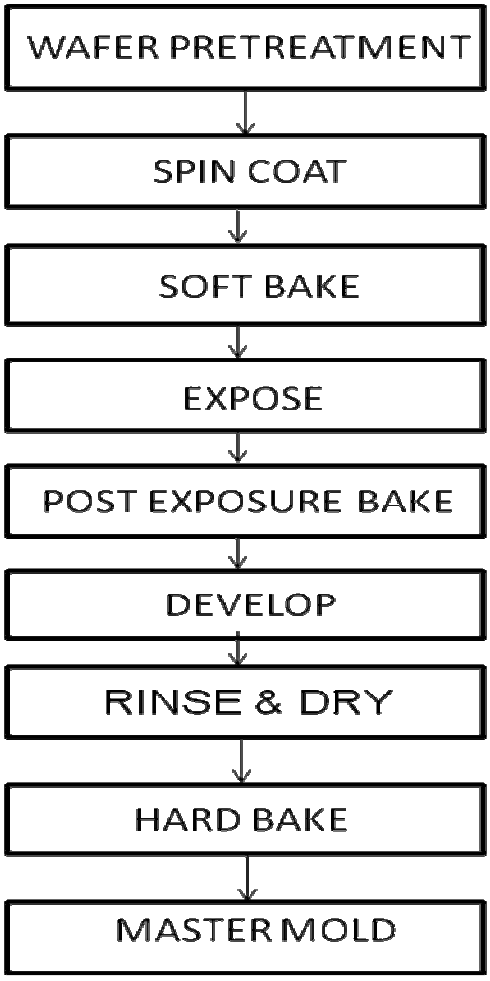

Figure 7: Flowchart showing the steps for fabrication of the master mold. These steps are carried out in clean room facility.

The next step is to spin coat the resist on the wafer. Wafer is held by the vacuum of the spinner chuck. Resist thickness is determined by the viscosity of the photo resist and the programmed speed of the coater. Spin coating step is carried out in two cycles namely, spread and spin cycle. During spread cycle, spin coater is ramped up to 500 RPM at 100rpm/sec acceleration for 5-10 seconds and during spin cycle ramped to final speed at an acceleration of 300rpm/sec for 30 seconds (SU-8). The final speed to achieve

a thickness of 15 microns using SU 8-5 is 1000 rpm/sec. It is 1000rpm/sec for thickness of 100 microns using SU 8-50. Table 1 shows the viscosities of the photoresist and the spin speed needed for respective desired thicknesses.

Table 1: The final ramp speed needed to get a desired thickness for a particular photoresist type.

Photo-resist Type	**Viscosity (cSt)**	**Desired thickness (µm)**	**Spin speed (rpm)**
SU-8 5	290	7	2000
		15	1000
SU-8 50	12250	100	1000

The prebaking step is carried out to get rid of the solvent from the resist and as such to densify it. This is two step process, lower initial bake temperatures allow the solvent to evaporate out of the film at a more controlled rate, which results in better coating fidelity, reduced edge bead and better resist-to-substrate adhesion. The higher temperature further solidifies the resist application. The wafer is prebaked at 65° followed by a higher temperature of 95°. Table 2 shows respective baking times for different resist thicknesses.

Table 2: Two step bake temperature for desired thickness and type of photoresist.

Photo-resist Type	**Thickness (µm)**	**Pre bake @ 65°** (minutes)	**Pre bake @ 95°** (minutes)
SU-8 5	7	2	5
	15	2	5
SU-8 50	100	10	35

After prebaking, the wafer is ready for alignment and exposure. Mylar mask is attached to a square glass plate, which is then positioned in the slot on Aligner. The coated wafer is placed on the wafer chuck. The Mylar mask is aligned with the wafer, so that the pattern can be transferred onto the wafer surface. Each mask, after the first one must be aligned to the previous pattern (two layers or more). Once the mask has been accurately aligned with the pattern on the wafer's surface, the photo resist is exposed. SU-8 is most commonly processed with conventional near UV (350-400nm) radiation. The substrate is exposured in contact geometry where the Mylar mask and wafer actually come in physical contact to give 1:1 feature reproduction. The interaction of resist with UV initiates a chemical reaction which yields a strong acid. Table 3 shows the exposure times for the desired thickness and the type of photoresist. The optimal exposure dosage depends on film thickness (thicker films require higher dosage) and process parameters.

Table 3: Exposure time needed for desired thickness and the type of photo-resist.

Photo-resist Type	**Thickness (μm)**	**Exposure time** (sec)
SU-8 5	7	11
	15	14
SU-8 50	100	36

Following exposure, a post expose bake (PEB) must be performed to selectively cross-link the exposed portions of the film. Optimum cross-link density is obtained by careful adjustment of the exposure and PEB process conditions. During post exposure baking (PEB), thermally driven and acid initiated reactions cross links the epoxy. As SU-8 is readily cross-linked, it can stress the film. To minimize the stress, wafer bowing

and resist cracking, two step contact hot plate process is done. Table 4 shows the baking time for different resist thicknesses.

Table 4: Two step post exposure bake temperatures for desired thickness and type of photoresist.

Photo-resist Type	**Thickness (µm)**	**Pre bake @ 65°** (minutes)	**Pre bake @ 95°** (minutes)
SU-8 5	7	1	1
	15	1	2
SU-8 50	100	1	10

After PEB, the wafer is ready to be developed. The wafer after cooling is immersed in developer and agitated till all the unexposed resist is washed out. Table 5 shows develop times for different thickness levels. These develop times are approximate, since the actual dissolution rates varies widely as a function of agitation rate, temperature and resist processing parameters.

Table 5: Development time needed for desired thickness and type of photo-resist.

Photo-resist Type	**Thickness (µm)**	**Exposure time** (minutes)
SU-8 5	7	1
	15	3
SU-8 50	100	10

The wafer is rinsed using isopropyl alcohol (IPA). At this step, if a white film is produced during rinse, this is an indication that the substrate has been under developed. The substrate is re immersed in SU-8 developer to remove the film and complete the development process and then dried completely by using nitrogen gun.

The final step is hard baking which enhances the mechanical strength of the resist. The wafer is hard baked at @ 65° for 2 minutes, @ 95° for 2 minutes, @ 150° for 20 minutes, @ 95° for 2 minutes and then @ 65° for 2 minutes. If it is a single layer process then the master mold is ready after this step else the wafer is recoated with the second layer and all the above processes are repeated again. Figure 8 shows a master mold with two devices on it.

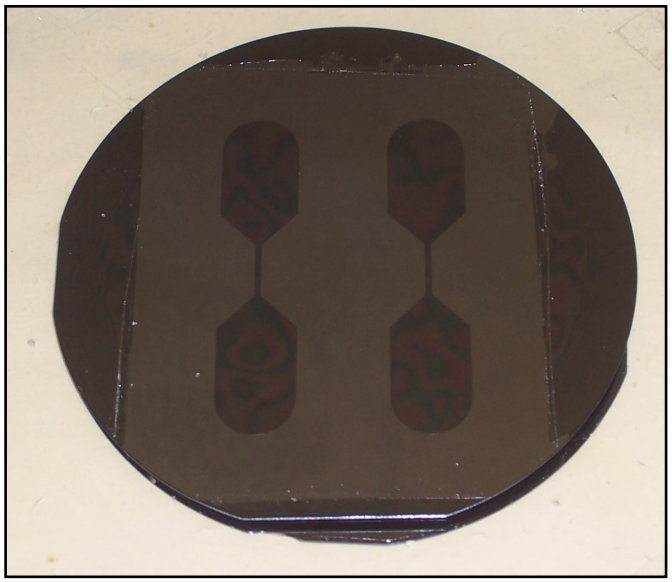

Figure 8: Photograph of a master mold showing the microfluidic device.

2.3 Casting PDMS Mold

Polydimethylsiloxane (PDMS) is used as a mold to make microfluidic devices. The fabrication is quite simple and economical to enable the production of single-use, disposable devices. PDMS device is transparent and can be bonded to glass cover slips, permitting placement on the stage of an inverted microscope and visualization of cells

during recording [18]. It is electrically insulating, chemically stable, environment friendly, biocompatible and impervious to gases.

A 4" silicon wafer with a pattern made out of SU-8 by photolithography is used to cast the polydimethylsiloxane (PDMS) microfluidic mold. Figure 9 shows the steps for making a microfluidic device from a master mold. The pre polymer and the curing agent are mixed in the ratio of 10:1. This PDMS mixture is desiccated in the desiccator which helps to remove bubbles formed during the mixing process [19].

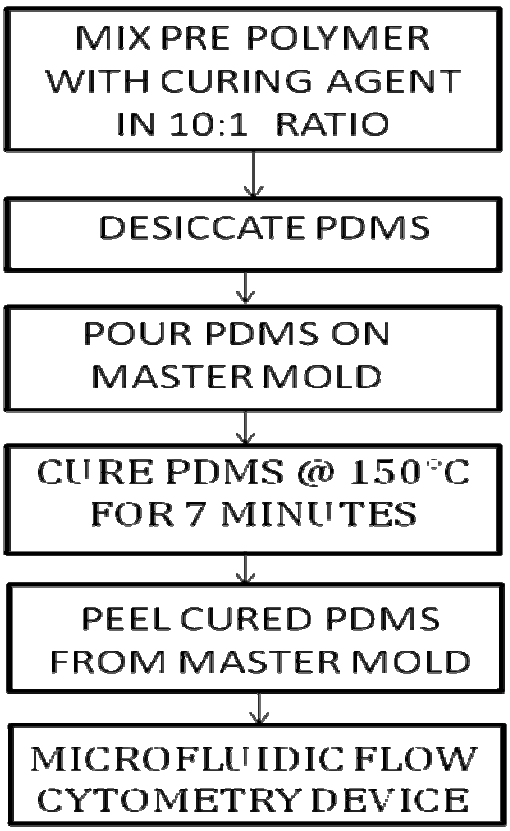

Figure 9: Flowchart showing the steps for fabrication of the PDMS devices from master mold.

The desiccated PDMS is poured on top of the wafer which is placed in an aluminum container. It is ensured that no bubbles are created in the process and if some small bubbles are created they are moved away from the device. PDMS is left undisturbed for some time till it uniformly spreads on the wafer. Eventually PDMS is cured at 150° for about 7 minutes. After curing, PDMS is left to cool down for few minutes. Then, using surgical knife the die is separated from the master mold. The master mold can be reused for making more PDMS based dies by following the same steps**.** Figure 10 shows the peeling of the cured PDMS devices from the master mold.

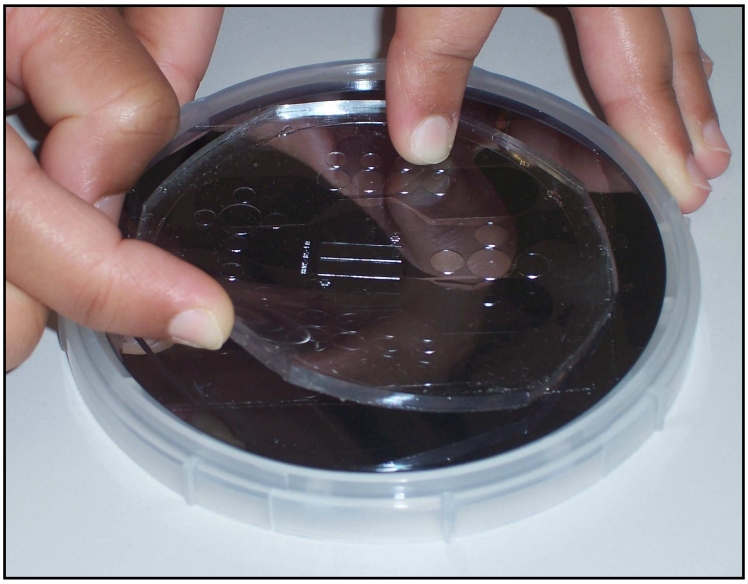

Figure 10: Peeling of the cured PDMS devices from the master mold.

2.4 Connecting Ports to Microfluidic Device

Once the PDMS molds (devices) are ready, the reservoirs are punched into the device using an appropriate size tissue biopsy punch. Then any debris are removed from the surface of the devices with the use of scotch tape. The devices are finally bonded to the microscopic glass slide/ coverslip with the help of hand held corona treater [20]. This

step not only makes the device bond to the glass, but also makes the device hydrophilic. To ensure that the devices stay hydrophilic, the devices are filled with the water and stored in aseptic conditions. Finally, when the devices are ready to use, stainless steel connectors with an outer diameter of 1.07mm are connected to the device through the site of punches created previously. Figure 11 shows the global view of the micro fluidic device with the input and output ports connected. Finally this assembly is placed across the micro fluidic circuit assembly consisting of microscope insert, suction system and pump to ensure continuity of fluid within the system**.**

Figure 11: Global view of the microfluidic device with the input and output ports connected.

CHAPTER 3

MICROFLUIDIC FLOW SETUP

3.1 Flow System Setup

One important component of a flow cytometer is a flow cell. Flow cell is a device or process through which liquid stream carries and aligns the cells so that they pass sample through the light beam for sensing. Flow cytometers are able to analyze several thousand particles every second in real time, and can actively separate and isolate particles having specified properties. A flow cytometer is similar to a microscope, except that instead of producing an image of the cell, flow cytometry offers "high-throughput" automated quantification of set parameters [8, 21].

These technologies are based on the manipulation of continuous liquid flow through microfabricated channels. Microfluidics is the handling and analyzing of fluids in structures of micrometer scale [15]. Actuation of liquid flow is implemented either by external pressure sources, external mechanical pumps, integrated mechanical micropumps, or by electrokinetic mechanisms.

Figure 12 shows the block diagram of the flow setup. The first block shows small volume delivery system. It holds the sample that is to be flown through the device. Tubing from this system is connected to the input port of the microfluidic device. Negative pressure is created by a peristaltic pump which pulls the liquid from the vial in the small volume delivery system into the microfluidic device.

Microfluidic device sits on the microscope as shown in the block diagram. As the sample moves through the channel, camera mounted on microscope captures the images. Sample then moves to the output port of the device to the tubing which is connected to one end of the pump. This pump eventually pulls this sample and it is collected as a waste.

The rotational speed of the pump pump rotates is controlled by the software interface (ULogger). It also controls the direction of rotation. Labjack, shown in above block diagram serves as an interface between peristaltic pump and computer. Images of sample are acquired through LABVIEW module from which video stream can be generated.

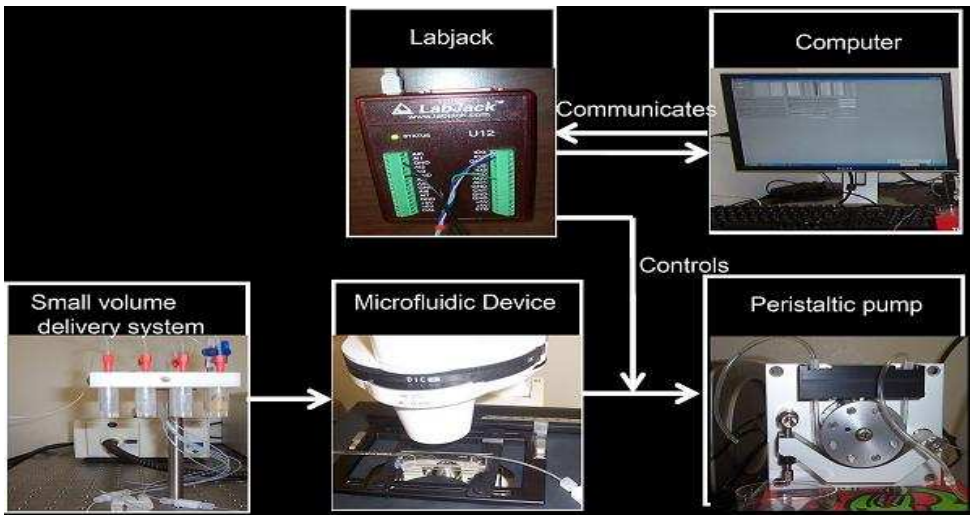

Figure 12: Block Diagram of the flow setup used for flowing sample through the microfluidic device.

3.2 Components of Flow Setup

This section discusses components of flow system in detail. It consists of small volume delivery system, microfluidic device integrated on microscope, peristaltic pump and labjack.

3.2.1 Small Volume Delivery System

The small volume perfusion system is used for sample delivery. Solutions can be either withdrawn using controlled flow systems or pushed by pressure. Peristaltic pump is used to pull the sample through the vial into the device. A common problem with the majority of available perfusion systems is that they have long lines of tubing which have to be filled before conducting experiments. This means that most of the sample will not contribute to the experiment and will be trapped in as a dead volume. This is not favorable because mostly the samples are expensive or are in limited quantities. This problem was overcome by the use of small volume perfusion system which drastically reduced the dead volume due to its smaller tubing size. This system utilizes small plastic tubes with conical bottom for holding the sample and thin Teflon tubing to connect to microfluidic ports. Figure 13 shows the picture of the small volume delivery system.

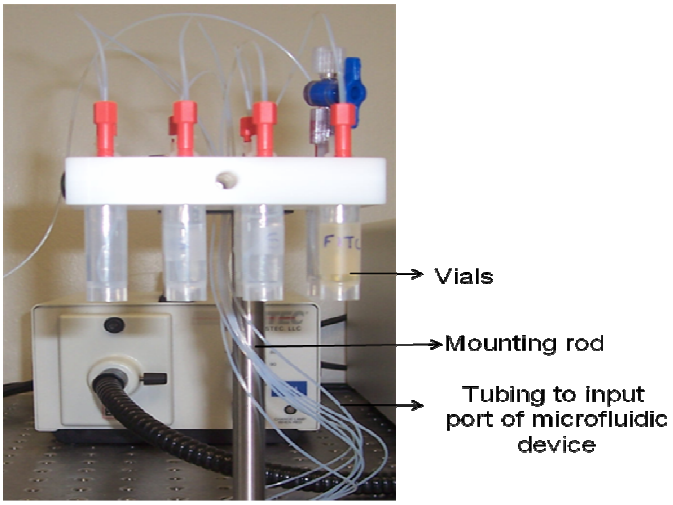

Figure 13: Small volume delivery system setup

The sample volumes of as low as 100 µl can be perfused with this system. The plastic vials with solutions can simply be threaded into the holder. Solutions can easily be refilled during the experiment by simply opening the pressure applicator connection. Because of its close proximity to the device, extra long tubing can be avoided and as such dead volume. The samples can also be switched in between the experiments. For this application the solutions are withdrawn by a negative pressure created by peristaltic pump.

3.2.2 Microfluidic Device

The holes were punched in the PDMS based dye using one millimeter biopsy punch. The device was then thoroughly cleaned using scotch tape. PDMS is hydrophobic by nature, this is a considerable drawback in microfluidic application since it renders the surface lacking in wettability with aqueous solvents and offers a channel surface prone to trapping air bubbles. This problem can be overcome by changing surface chemistry of PDMS which was done by treating the device with hand held corona treater. This step not only made the device hydrophilic but also irreversibly bonded the PDMS to the glass slide. It was important to bond the device to the glass because pressure was applied to drive the flow through the device. The reversible bonding resulted in leakage through the device after sometime. To overcome this problem, devices were permanently bonded to the glass. After the devices were bonded, they were filled with water to maintain the hydrophilicity and then stored in sterile conditions.

Eventually when the devices were to be used, the input and output ports were connected to the devices. The stainless steel connectors with 90^0 bend were used as ports.

The outer diameter (OD) of these connectors is 1.27 mm. So these connectors made a good fit within one millimeter hole in PDMS as PDMS is flexible polymer. But we had to be very careful during inserting these connectors because a slight offset was causing the back flow through the connector. So this step is very crucial to avoid any leakage from the device. Then the tubings are connected to the input and output ports of the device. The microfluidic device fabricated for this application consists of 3 basic designs:

Microfluidic device design 1: It is a single channel connected by two reservoirs. The depth of reservoir as well as channel was 100 μm. The channel was 1000 μm in width and 10000 μm in length. Figure 14 shows global view of the device and zoomed in channel.

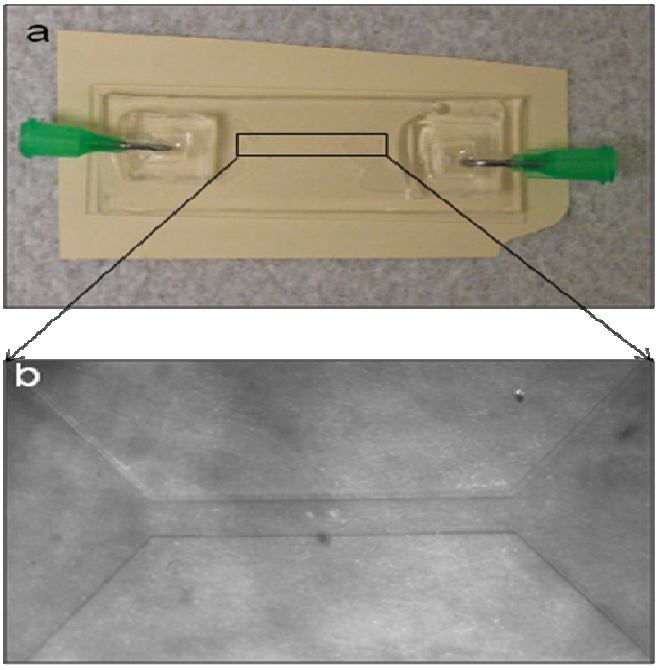

Figure 14: Microfluidic device design 1. (a) Global view of the device with input and output ports connected (b) zoomed in channel.

This device offered less fluidic resistance. But this device is not ideal for flow cytometry because cells flow in different planes due to large dimensions of the channels. As such it was not possible to interrogate single cell at a time. This device however, helped in understanding the challenges and difficulties of flowing fluid through microfluidic devices. Images and videos of fluorescein, fluorescent beads and epithelial cells were acquired through this device.

Microfluidic device design 2: This was again a single channel connected by two reservoirs. But here reservoir and channel had a depth of 100 μm and 15 μm respectively. The channel was 1000 μm in width and 10000 μm in length. Images and videos of fluorescein, fluorescent beads and epithelial cells were acquired through this device. Figure 15 shows global view of the device and zoomed in channel.

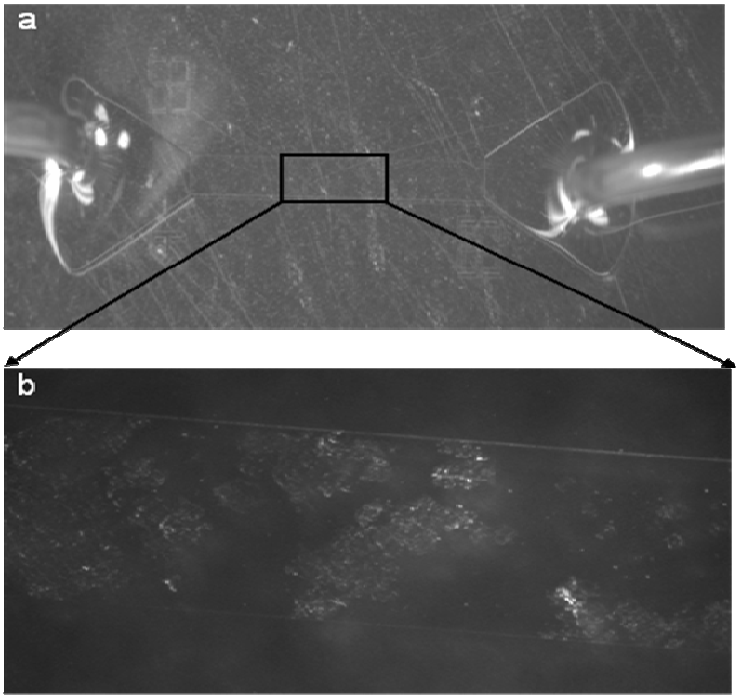

Figure 15: Microfluidic device design 2. (a) Global view of the device with input and output ports connected (b) zoomed in channel.

Microfluidic device design 3: This device had multiple channels connected by two reservoirs. The reservoir and channel depth was 100 μm and 7 μm respectively. Each channel was 10 μm in width and 10000 μm in length and separated by 50 μm. Images and videos of fluorescein and epithelial cells were acquired through this device. Figure 16 shows global view of the device and zoomed in channels.

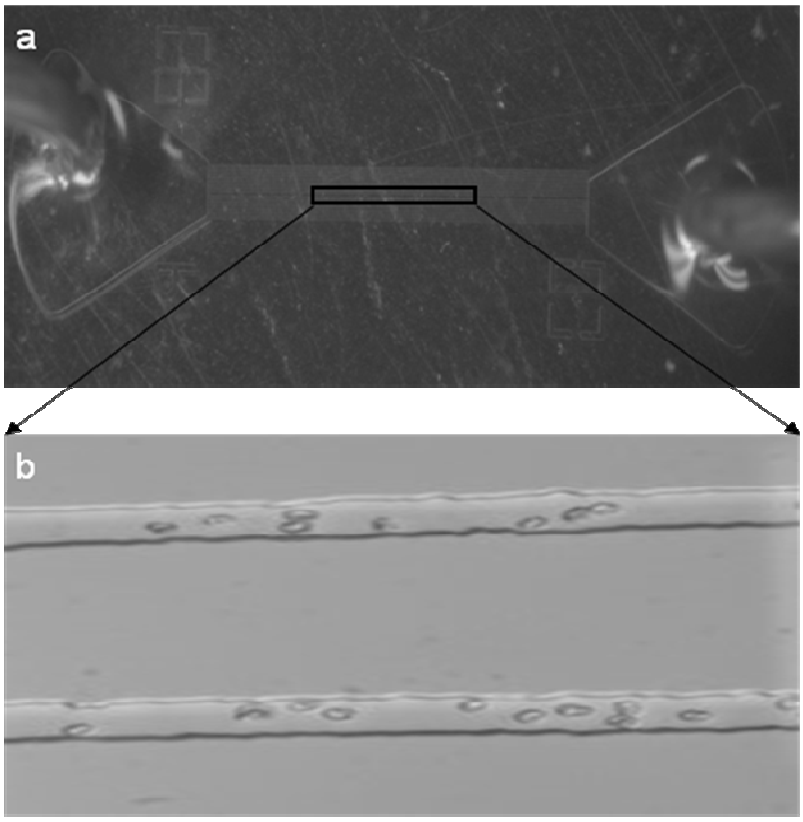

Figure 16: Microfluidic device design 3. (a) Global view of the device with input and output ports connected (b) zoomed in multiple channels.

To start with the devices are flushed by Triton X (non ionic surfactant) to make the surface hydrophilic. Making surface hydrophilic, offers less resistance to the fluid and as such smooth flow. This technique of using surfactant to make devices hydrophilic is not recommended if live cells are to be used. Moreover using surfactant generates

bubbles in the microfluidic platform which eventually becomes difficult to get rid of. Alternatively, Trintron X can be used to make the surfaces hydrophilic. Once the devices are hydrophilic in nature, water is flushed through them to get rid of any remnants. Now the device is ready to flow any sample.

The entire microfluidic device sits on a microscope to enable real-time imaging of sample through the device. Figure 17 shows the microfluidic device with ports integrated on the microscope for visualization. For imaging fluorescent beads and fluorescein, the fluorescent X cite source in combination with appropriate filter set was used to image them through the microfluidic device. For imaging epithelial cells, microscope was used in differential interference contrast (DIC) mode and videos were acquired.

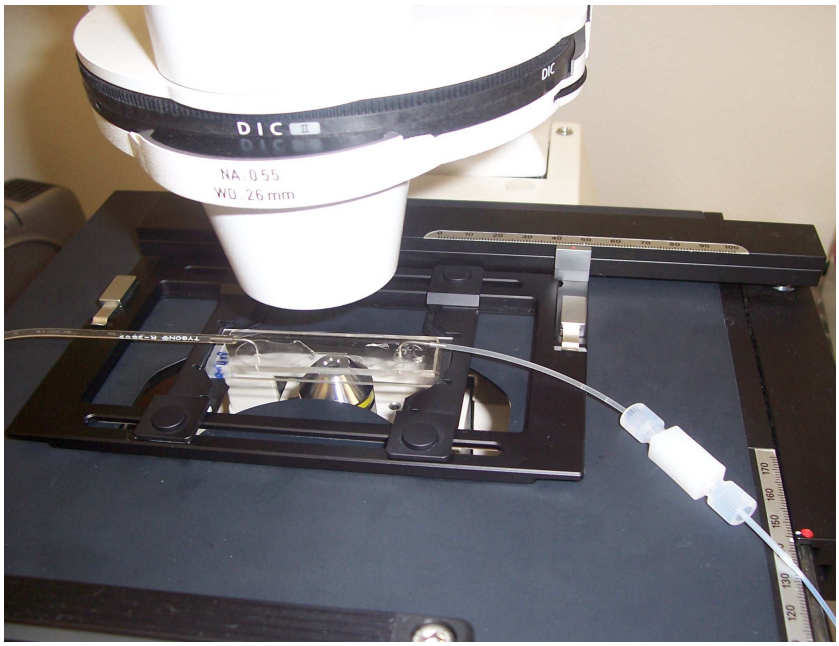

Figure 17: Microfluidic device integrated on the microscope with input and output ports connected.

3.2.3 Peristaltic Pump

It is a type of displacement pump used for pumping a variety of fluids. The fluid is contained within a flexible tube fitted inside a circular pump casing. Eight rotors attached to the external circumference compress the flexible tube (Figure 18). As the rotor turns, the part of tube under compression closes (or 'occludes') thus forcing the fluid to be pumped to move through the tube. It is a four channel system, can go in clockwise as well as anticlockwise direction. The flow rate can be set anywhere from 0.07 ml/min/channel to 150 ml/min/channel and can withstand a pressure till 65 psi.

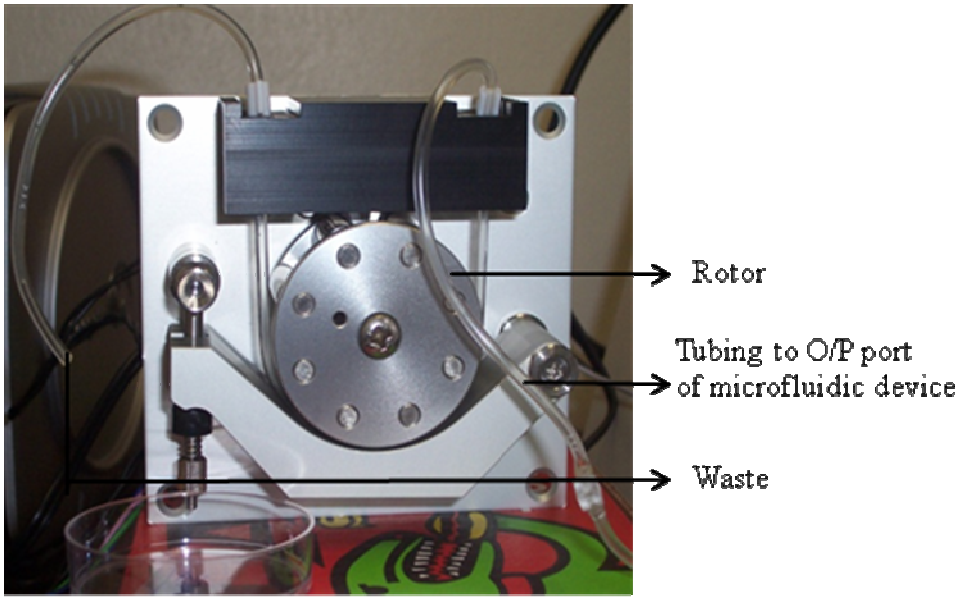

Figure 18: Peristaltic pump used to create negative pressure in the microfluidic device for allowing suction of fluid.

3.2.4 Labjack

LabJack is a measurement and automation peripheral that enables the connection of a PC to the real world. This LabJack is USB based measurement and automation devices which provide analog inputs/outputs, digital inputs/outputs, and more. They serve

as an inexpensive and easy to use interface between computers and the physical world. It acts as an interface between the peristaltic pump and the computer.

3.3 LABVIEW Module for Video and Image Acquision

Front panel shown in figure 19 is a LABVIEW interface used for acquiring videos of flowing cells, beads and fluorescein. For video, 30 frames per second are captured. Time for which video is to be acquired is entered by user in 'Time Target' slot. Time entered is in seconds.

Figure 19: Front panel of LABVIEW VI for acquiring images of flowing beads, cells and fluorescein.

CHAPTER 4

OPTICAL SETUP FOR IMAGING

The morphology of cells can be important in many contexts. In culture the morphology indicates the status of the cells, both in terms of the health of the cells and in the case of primary isolates the differentiation state may be critical. Cell morphology detection can allow to measure cell size, cell symmetry, nuclear size and nuclear density. These parameters will allow identifying healthy cells from abnormal cells such as in cancerous cell detection. It flow cytometer for urine analysis morphology detection studies will help in identifying different cells present in urine as well as morphological changes occurring due to illness.

To detect these changes, a highly sensitive technique is needed. The technique proposed here for low coherence interferometric technique is DPCI. It is a differential phase contrast interferometic technique in which high phase resolution is achieved by employing two interferometric channels and eliminating common mode noise due to environmental factors by making a differential measurement. Distinguishing features of DPCI instrument include its high speed and being fiber based. These two features are very important for high throughput screening of cells and robust integration with a microfluidic chip.

4.1 Differential Phase Contrast Interferometer (DPCI)

The prototype DPCI system is a novel dual channel low coherence Michelson interferometer constructed using polarization maintaining (PM) optical fiber (Figure 20) that is capable of differential phase measurement between light backscattered from two spatially separated sites in a specimen [22]. The two channels correspond to orthogonal polarization modes of the PM fiber. At the interferometer input, light emitted from a broadband source (λ_o=1.31 μm, $\Delta\lambda$=60 nm) is coupled into a Lyot depolarizer which gives two independent and decorrelated linearly-polarized modes that propagate along the birefringent axes (fast and slow) of the PM fiber and form Channel 1 (Ch1) and Channel 2 (Ch2).

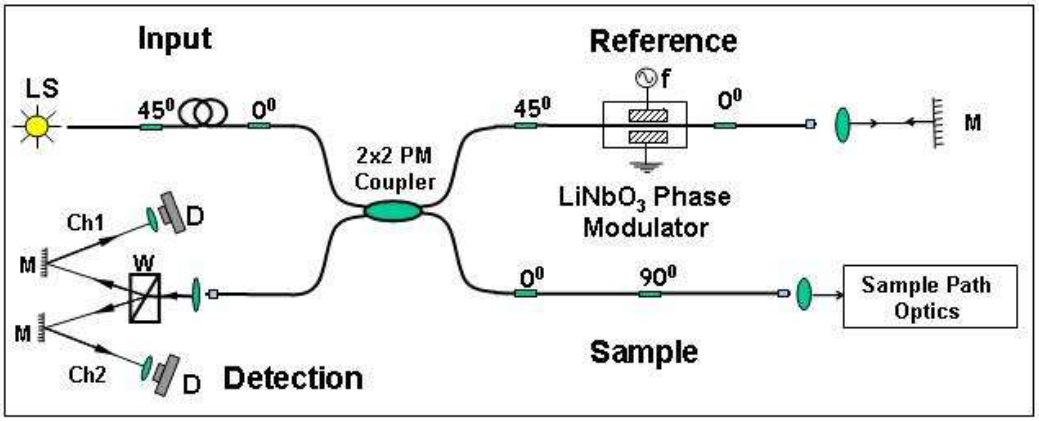

Figure 20: Prototype (DPCI) system constructed using polarization maintaining (PM) fiber.

Decorrelation of the two polarization modes is an important feature of the DPCI system as it ensures that cross-coupled light from one channel to the other does not contribute to the interferometric signal in either channel. Light amplitudes in each channel divide nearly equally into reference and sample paths at the PM fiber coupler.

Back reflected light from the reference and sample mix at the PM coupler to form interference fringe intensity signal signals in Ch1 (I_1) and Ch2 (I_2).

For phase contrast imaging with DPCI system, two configurations of sample path optics to spatially separate DPCI probe beams (figure 21) corresponding to Ch1 and Ch2 can be employed. DPCI has a demonstrated sensitivity of 0.1 nm in measuring changes in optical path length. In either case, the DPCI measures the optical path length difference between the two spatially separated locations of the probe beams. The tips of the arrows of the probe beams in either configuration indicate the interface used for reflecting light back into the interferometer. In a differential phase measurement, $\Delta\varphi$ is proportional to difference in optical path length (Δ p) traversed by light in Ch1 and Ch2 (Eq. 2).

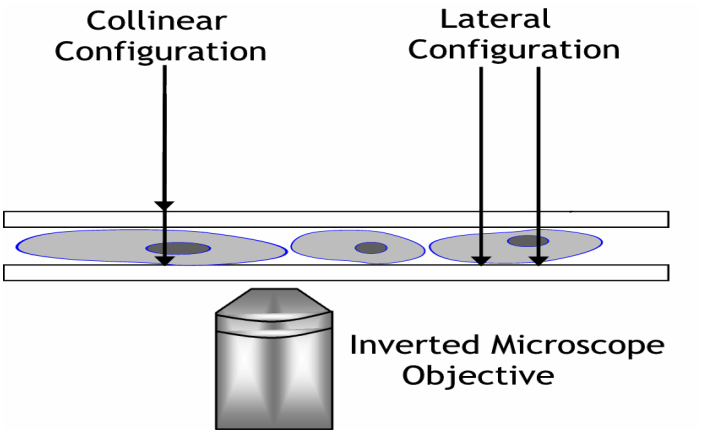

Figure 21: Sample path configuration for recording brightfield and *en face* DPCI

Factor of two in Eq. 2 accounts for double pass geometry. Δp is a function of refractive index variation (Δn) and physical path length difference (l) between Ch1 and Ch2 and can be written as,

$$\Delta\varphi = 2\left(\frac{2\pi}{\lambda_o}\right)\Delta p \qquad \text{Eq. (1)}$$

$$\Delta p = \int \Delta n(l) dl \qquad \text{Eq. (2)}$$

The sample holder is mounted on a computer controlled linear motorized XY translation stage. Cells to be imaged with DPCI are first visualized with an inverted microscope placed underneath the sample holder as shown in figure 21. A 40× objective lens was used to focus DPCI sample beams to a spot diameter of 3.5 μm. In these experiments, a both lateral and collinear configuration for en face DPCI imaging of cells was done. Synchronous movement of motorized linear translation stages in the XY plane does *en face* imaging of the specimen. Interference fringe intensity signal (I_m) in each channel is recorded while the specimen is translated along the X-direction, which constitutes a single line scan. Stacking processed individual line scans gives an *en face* DPCI image of the cell layer.

DPCI has unique capabilities to measure changes in optical path length with unprecedented accuracy and sensitivity. In a sample the optical path length is a product of its refractive index and geometrical length. The sub-nanometer sensitivity in measuring changes in optical path can be uniquely exploited for applications involving cells which include quantitative morphometry of cells without the use of any stains or labels. Precise quantification is critical in automated screening for cells. For example, cell nuclear density is the single most important morphological biomarker that differentiates normal cells from the cancerous ones. As samples are not labeled they can be used for further analysis using other methods.

CHAPTER 5

RESULTS

At the microscale, different forces become dominant over those experienced in everyday life. New designs are made to take advantage of forces that work on the microscale. The effects that become dominant in microfluidics include laminar flow, diffusion, fluidic resistance, surface area to volume ratio, and surface tension [15]. To understand some of these flow characteristics, fluorescein, beads and epithelial cells were observed as they moved through microfluidic devices. These tests were performed using three different microfluidic devices as described in chapter 3.

Depth measurements of microfluidic devices fabricated using soft lithography technique were measured using Optical Coherence Tomography (OCT). It was important to know whether the fabrication recipes were actually giving the targeted depths.

Flow rate within a channel can be calculated by using a formula $Q = \Delta P / R$ where Q is flow rate, ΔP is the pressure drop across the channel and R is the channel resistance. Also, microfluidic devices used for this application have a rectangular geometry. The resistance of a rectangular channel with high aspect ratio ($w >> h$ or $w << h$) is given by,

$$R = \frac{12\mu L}{wh^3}$$

where w is channel width, h is channel height, μ is fluid viscosity and L is length of a channel [15].

Fluorescein was chosen as a sample to flow through device because it was easy to visualize under fluorescent microscope. Fluorescein is a fluorophore commonly used in microscopy. Fluorescein has an absorption maximum at 494 nm and emission maximum of 521 nm. This set of experiments indicated how robust these devices were fluidically.

Suncoast yellow fluorescent beads having excitation wavelength of 540nm and emission of 600nm were also observed flowing through device. 10µl of beads were aliquot in 3 ml of DI water. These beads had a mean diameter of 9.91 µm. Fluorescent microscope was used to visualize these beads as they flowed through the device.

Mucosal epithelial cells suspended in Phosphate Buffer Saline (PBS) were also used as a sample to flow through devices. These cells were obtained from cheek. DIC microscope was used to visualize these cells.

5.1 Characterization of microfluidic devices

The channel and reservoir depths were measured using sensitive technique of Optical Coherence Tomography. It was important to characterize these devices to know if they were actually resulting in desired depths. It was found that there was actually an error between desired and actual depths. Table 6 summarizes the results for the same.

Table 6: Characterization of microfluidic device.

Desired Thickness(µm) Soft Lithography	**Actual Thickness (µm) OCT**	**Error(%)**
15	18	20
100	158	37

5.2 PDMS modified surface hydophilicity test

After the devices were treated with corona for making devices hydrophilic, it was important to monitor how long they stayed hydrophilic. Hydrophilic nature of PDMS devices not only makes fluid flow smooth (offers less resistance) but also avoids bubble formation in devices.

One important parameter that helped in determination of extend of hydrophilicity/hydrophobicity is measurement of contact angle. Contact angle is the angle at which this liquid drop meets the PDMS. Immediately after treating devices with corona, water droplet spread out (contact angle 0^0) on PDMS surface indicating a hydrophilic surface. Contact angle increased with time and after about 25 minutes the device had lost its hydrophilic property. Some devices after treatment were filled with water and they retained their hydrophilic surface property.

5.3 Microscopic images of flowing sample

5.2.1 Images from device 1

It was a single channel connected by two reservoirs. The depth of reservoir as well as channel was 100 μm. The channel was 1000 μm wide and 10000 μm in length. Aspect Ratio for this device was 10:1 (width of channel versus depth of channel). Flow rate was varied from 0.07 ml/min to 2 ml/min and device was found to be fluidically robust. This device offered minimal resistance and as such flow through device was smooth. Suction was created in the device by peristaltic pump which forced fluorescein to flow from input to output port. 2 millimolar solution of fluorescein was made by mixing it in water. Figure 22 shows images of fluorescein flowing through this device. Figure

22a and 22d shows the dye in input and output reservoir whereas figure 22b and 22c shows fluorescent dye in channel at two different locations.

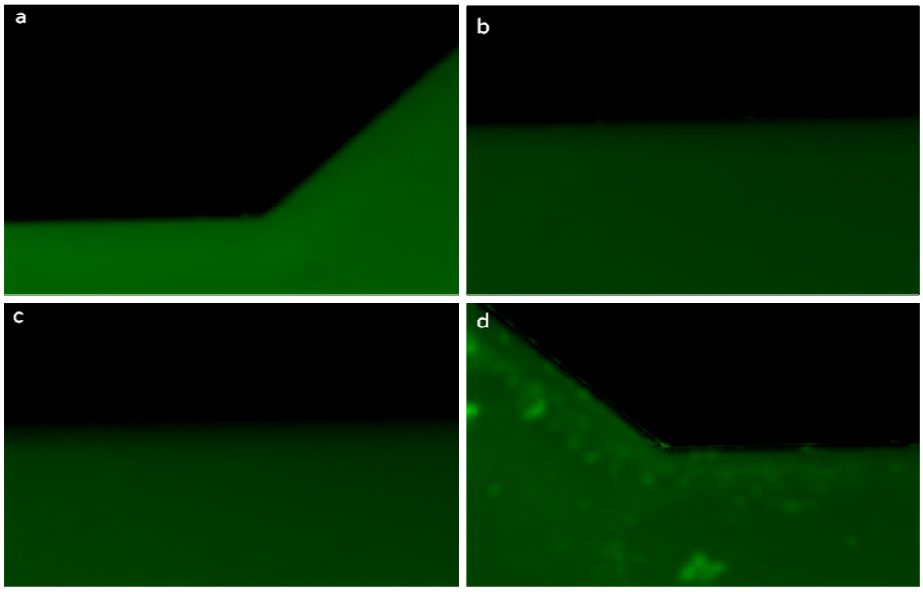

Figure 22: Fluorescein in device # 1. a) fluorescein in input reservoir b) & c) fluorescein in channel d) fluorescein in output reservoir.

As the channel depth of this device was 100 μm, beads travelled in different planes. Figure 23, shows beads flowing through device. This figure shows red streaks which signifies that beads are traveling at high speed. Speed of beads was varied from 0.07 ml/min to 2 ml/min. Integration time for these images were 1.25 seconds and was captured at magnification of 10x. It was also observed that beads flowed at different velocities across the cross section of channel. Many beads lined up along the edge of the channel. Figure 23a shows beads flowing in the reservoir whereas figure 23b show beads flowing in channel.

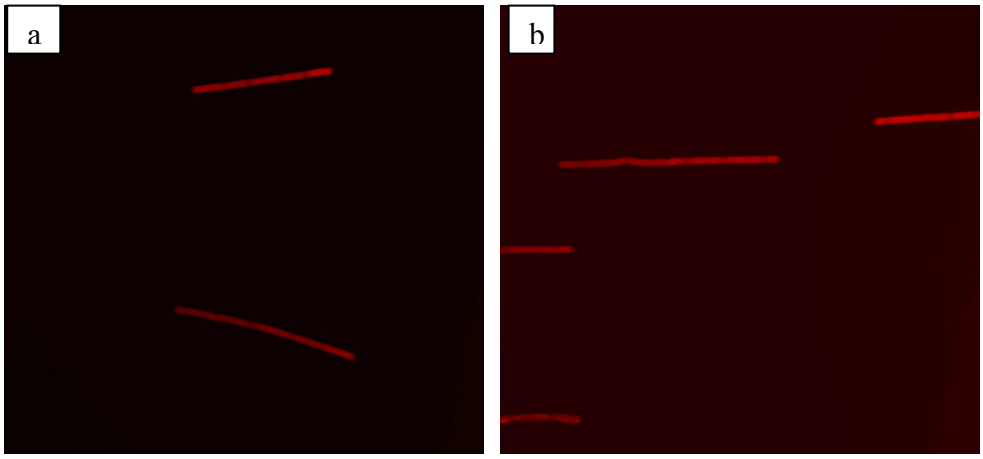

Figure 23: Fluorescent beads in device # 1 a) beads in reservoir b) beads in channel.

Cells were also made to flow through this device at variable flow rates ranging from 0.07 ml/min to 2 ml/min. These cells had tendency to move as a group, although some cells also flowed without clustering together. Figure 24a shows cells in channel and figure 24b shows cells in reservoir.

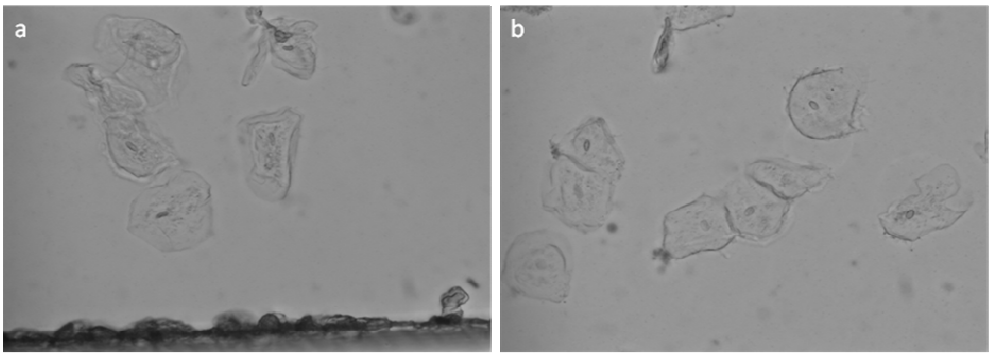

Figure 24: Epithelial cells in device # 1 a) cells in channel b) cells in reservoir.

5.2.2 Images from device 2

This was a single channel connected by two reservoirs. But here reservoir and channel had a depth of 100 μm and 15 μm respectively. The channel was 1000 μm in width and 10000 μm in length. The aspect ratio for this device was 67:1 (width of

channel versus depth of channel). Concentration of dye used was 4 millimolar and flow rate was set all the way from 0.07ml/min to 2 ml/min. This device offered higher resistance as compared to device 1 and as such flow through device was not smooth.

Figure 25 shows images of fluorescein flowing through this device. Figure 25a and 25d shows the dye in input and output reservoir whereas figure 25b and 25c shows fluorescent dye in channel at two different locations. As seen from figure 25d, majority of times leakage was detected from this device. This could be due to higher flow rate through the device. Also, intensity of fluorescein appears more in reservoir as compared to that in the channel. It is because of more fluorophores present in reservoir due to its higher depth (100 μm) as compared to that of a channel (15 μm).

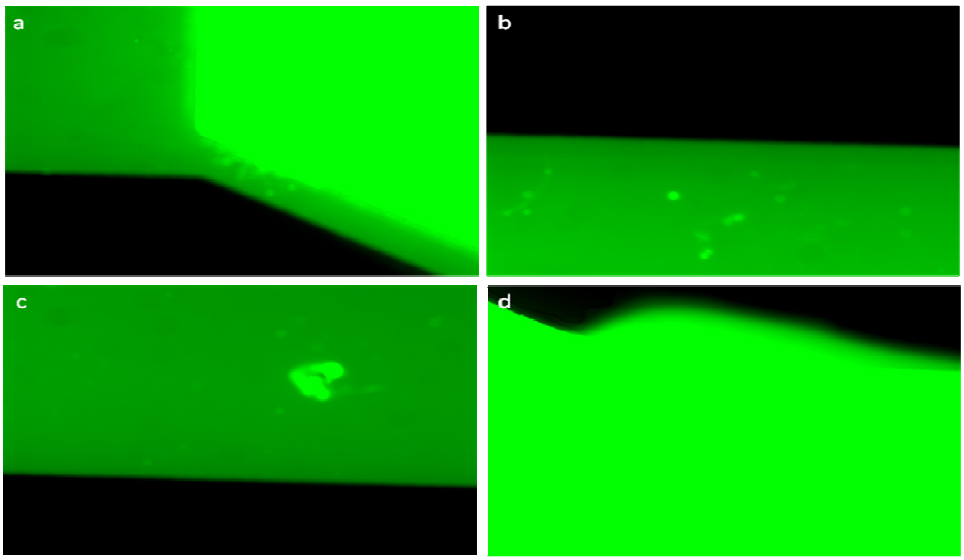

Figure 25: Fluorescein in device # 2 a) fluorescein in input reservoir b) & c) fluorescein in channel d) fluorescein in output reservoir.

Fluorescent beads (540,600) were made to flow through this device. As beads had a mean diameter of 9.91 μm and this device had channel of 15 μm depth. It was expected that beads would flow as a single sheath. But majority of the beads got stuck at the

interface between reservoir and channel. There could be number of reasons for this. Firstly, it is possible that there were some beads larger that channel depth that got trapped. Secondly, there could be some surface chemistry between these beads that made them aggregate and hindered their flow through channel. As such further flow was prevented, no matter what flow rate was used. As streaks of beads are not seen, it represents that beads are almost stationary. Figure 26a shows beads in the channel, just next to reservoir. Figure 26b and 26c shows beads stuck at the interface which subsequently prevented any beads to flow. Figure 26d shows some beads that made it to the channel.

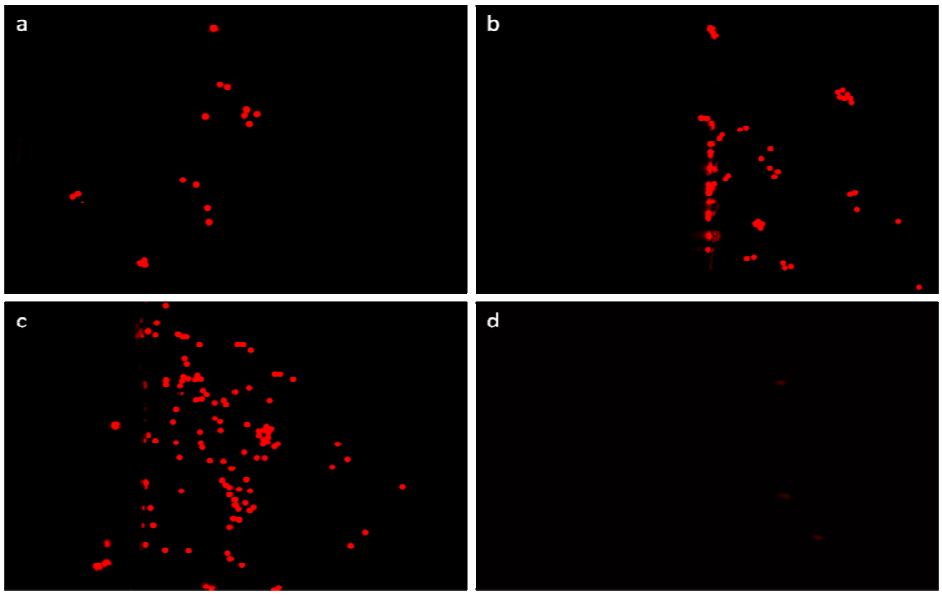

Figure 26: Beads in device # 2 a) beads in channel (next to reservoir) b) & c) beads stuck at interface between reservoir and channel d) fluorescein in channel.

Mucosal epithelial cells suspended in Phosphate Buffer Saline (PBS) were also flown through device. Cells were made to flow through this device at higher flow rate. Again most of the cells got stuck at the interface and as such stopped the flow in the channel. Figure 27a shows cells in channel and figure 27b shows cells in reservoir.

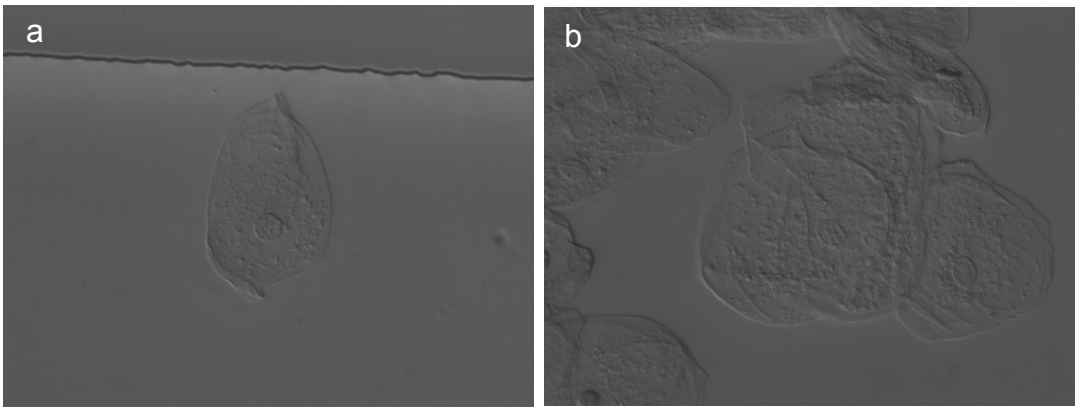

Figure 27: Epithelial cells in device # 2 a) cells in channel b) cells in reservoir.

5.2.3 Images from device 3

This device had multiple channels connected by two reservoirs. The reservoir and channel depth was 100 μm and 7 μm respectively. Each channel was 10 μm in width and 10000 μm in length and separated by 50 μm. Aspect ratio calculated was this device was 143:1. Fluorescein was made to flow through this device as well. This device offered much higher resistance as compared to device 1 and device 2 and as such flow through device was not smooth. Figure 28 shows images of fluorescein flowing through this device. Figure 28a and 28d shows the dye in input and output reservoir whereas figure 28b and 28c shows fluorescent dye in channels at two different locations. As seen from figure 28b, some of the channels didn't let fluorescein to flow through. This could be due to manufacturing defect of the device. Also, intensity of fluorescein appears much more in reservoir as compared to that in the channels. It is because of more fluorophores present in reservoir due to its higher depth (100 μm) as compared to that of a channel (7 μm)

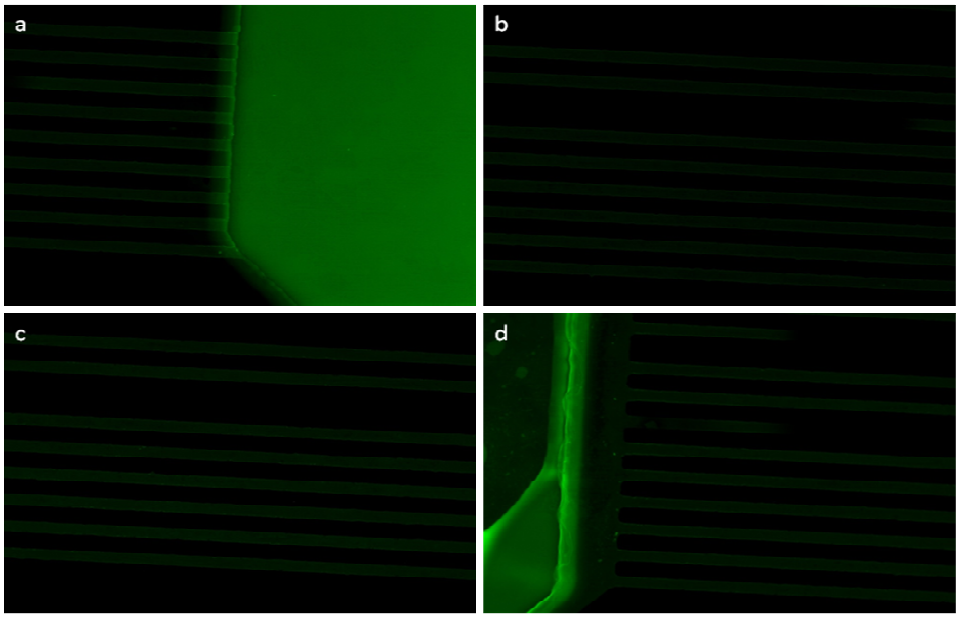

Figure 28: Fluorescein in device # 3 a) fluorescein in input reservoir b) & c) fluorescein in channels d) fluorescein in output reservoir.

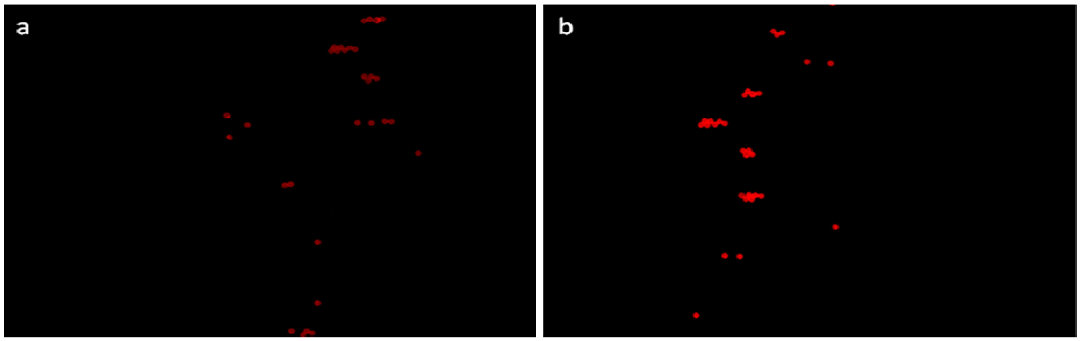

Figure 29: Beads in device # 3 a) & b) beads lined up and stuck in channel (next to reservoir)

Beads made to flow through this device also had a mean diameter of 9.91 µm, but as channel was just 7 µm depth, it was expected that beads would not enter channels due to dimension constraint. But some of the beads actually entered channels and eventually got stuck, preventing further flow. The possible reasoning for this is either channels had

higher depth than they were fabricated for or some of the beads were actually smaller than 7 μm that made them enter channel. Figures 29a and 29b, both show beads in the channel, just next to reservoir. Nothing was seen on the output reservoir.

Epithelial cells were not made to flow through this device because width of channel was just 10 microns, where as for epithelial cells to pass through, these channels should have been much wider.

5.4 Images obtained from DPCI setup

En face DPCI images quantitatively map the variation of optical path length in cells. Poor reflectivity/absorption contrast of epithelial cheek cells makes visualization difficult with a bright field microscope. Figure 30 shows DPCI image of multiple epithelial cheek cells and also phase contrast microscope image of similar epithelial cheek cells

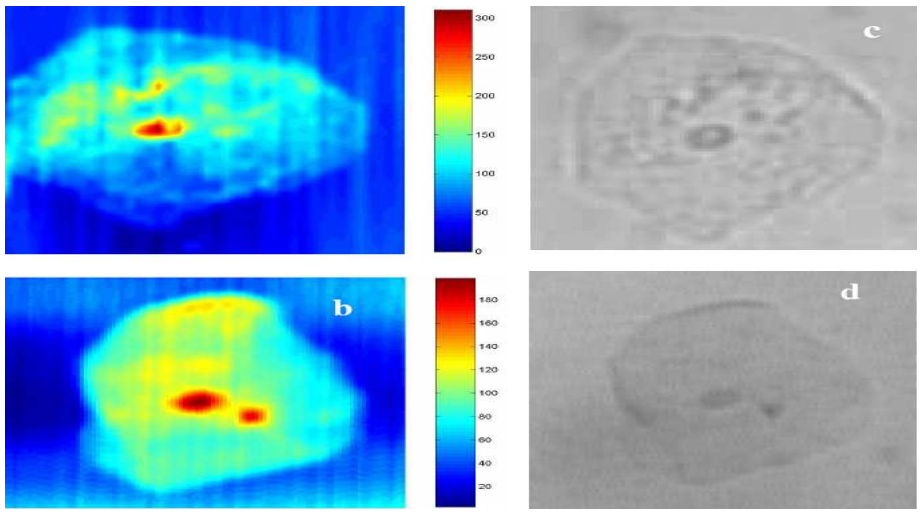

Figure 30: DPCI (**a** & **b**) and bright field microscope images (**c** & **d**) of single human epithelial cheek cells. Lateral (**a**) and collinear (**b**) probe beam configuation were used to record DPCI images. Color bar denotes optical path length in nanometers.

CHAPTER 6

DISCUSSION AND CONCLUSIONS

Characterization of microfluidic devices from fluidic and imaging standpoint is very critical. As seen from the results of device characterization, there is error in the depths of the devices. The devices are having higher depth than they are fabricated for. The devices not only had higher depth than desired but also increase in the radial dimensions. So, a channel fabricated for a depth of 15 microns and width of 10 microns actually resulted in a depth of 18 microns and width of 15 microns. The extension in the width is a limitation of the Mask aligner that is used. So, this problem can be handled by designing a device with lower width than desired so that after fabrication an accurate width can be expected. For getting an accurate depth again some parameters in the fabrication process have to be manipulated to reduce the error.

PDMS by nature is hydrophobic and for flow cytometry this is an undesirable characteristic. The device has to be fluidically robust so that continuous interrogation of the cells can be achieved. The hydrophobic surfaces tend to increase fluidic resistance and also create bubbles both of which cannot be afforded in this setup. So, either devices need to be used within half an hour after treatment or else filled up with water and stored. This will make sure that devices stay hydrophilic and hence not hinder in fluid flow or imaging.

The three microfluidic devices discussed for this application have to be further optimized for robust fluidic setup. As seen from the results, some of the devices were not apt for flowing beads or cells through them. For imaging cells, it is important that a single sheath of cells flow through the interrogation point or else it will generate erroneous results.

Unlike conventional flow cytometer where only one cell flows through the point of interrogation these two flow cytometer designs permit interrogation of several cells as the probe beams scan the flow channel which will substantially improve the throughput. The throughput (TP_{cell}) of the DPCI instrument integrated with microfluidic flow cytometer can be calculated by,

$$TP_{cell} = \frac{N \times 2 f_s \times d}{s} \qquad \text{Eq. 3}$$

where N is the average number of cells flowing through the detection line, f_s is the operating frequency of the resonant galvo, d is the spot size of the probe beam, and s is the average diameter or length of the cell. A factor of two appears in eq 3 since two line scans are (back and forth) completed in one frequency cycle. N will depend on the flow rate of cells in the microfluidic chip flow channel and the spacing between cells as the detection point. DPCI instrument is not a limiting factor for high throughput analysis. The factors that will limit the throughput are the galvo speed and the maximum cell flow rate that can be achived in the microfluidic flow cytometer.

CHAPTER 7

FUTURE GOALS

Cells communicate through a network of different substances, including cytokines, interleukins, and hormones. The secretion of such substances reflects the functional state of the cells and is programmed by gene expression. In the case of tumor cells, the progression to states of increasing malignancy is accompanied by changes in gene expression. Peptides or proteins that are secreted by cancer cells in different states of progression could be possible candidates in the search for new biomarkers.

Surfaced Enhanced Raman Spectroscopy (SERS) can be integrated to the current setup to detect the presence of multiple molecular markers using functionalized gold nanopartcles with attached Raman reporter dyes indicative of specific cell molecular biomarker antibody. SERS detection will be done in the output reservoir port of the microfluidic chip. A multimode fiber with a lens attached to its tip will be positioned next to the port which will carry excitation and scattered SER signal from the gold nanotags to a Raman spectrometer. SERS detection cannot be done on individual cell since the integration time necessary to collect SERS signal far exceeds the dwell time of the cell in the flow channel.

APPENDIX A

SOFTWARE INTERFACE

Software interface for controlling various parameters of the peristaltic pump. Analog Out 0 controls the speed of pump. IO state write controls direction of the pump, clockwise or anticlockwise. The flow rate can be set anywhere from .01 ml/min to 150 ml/min. It can be configured for 8 channels

REFERENCES

[1] C. BD, "Clinical utility of body fluid analyses," *Clinics in Laboratory Medicine,* vol. 5, pp. 195-208, 1985.

[2] D. I. Szamosi, J. M. Bautista, J. Cornbleet, L. Glasser, G. Rothe, L. Sandhaus, M. Key, A. Meloni-Ehrig, N. B. Culp, and W. Dougherty, "Body Fluid Analysis for Cellular Composition; Approved Guideline," *Clinical and Laboratory Standards Institute (CLSI).* vol. 26, pp. 1-97, 2006.

[3] J. A. Simerville, W. C. Maxted, and J. J. Pahira, "Urinalysis: A Comprehensive Review," *American Family Physician,* vol. 71, pp. 1153-1162, 2005.

[4] S. S. Raab, D. M. Grzybicki, C. M. Vrbin, and K. R. Geisinger, "Urine Cytology Discrepancies: Frequency, Causes, and Outcomes," *American Journal of Clinical Pathology,* vol. 127(6), pp. 946-953, 2007.

[5] H. Nakamoto and T. Okada, "Apparatus for analyzing cells in urine," US: TOA Medical Electronics Co., Ltd, 1997, pp. 1-9.

[6] Noushin Shayanfar, U. Tobler, A. v. Eckardstein, and L. Bestmann, "Automated urinalysis: first experiences and a comparison between the Iris iQ200 urine microscopy system, the Sysmex UF-100 flow cytometer and manual microscopic particle counting," *Clin Chem Lab Med* vol. 45, pp. 1434-1439, 2007.

[7] J. P. Houston, M. Naivar, J. C. Martin, G. Goddard, S. Carpenter, J. R. Mourant, and J. P. Freyer, "Endogenous fluorescence lifetime of viable cells by flow cytometry," *Proc. SPIE,* vol. 6859, pp. 1-8, 2008.

[8] J. Wietzorrek, M. Stadler, and V. Kachel, "Flow Cytometric Imaging - a novel tool for identification of marine organisms," *IEEE,* vol. 7803 pp. 688-693, 1994.

[9] E. Martz, "Introduction to Flow Cytometry," Amherst: University of Massachusetts, 2000, pp. 1-3.

[10] W. K. Wu, C. K. Liang, and J. Z. Huang, "MEMS-Based Flow Cytometry: Microfluidics-Based Cell Identification System by Fluorescent Imaging," *IEEE,* vol. 26, pp. 2579-2581, 2004.

[11] A. Star, J. N. Eugene Tu, J.-C. P. Gabriel, C. S. Joiner†, and C. Valcke, "Label-free detection of DNA hybridization using carbon nanotube network field-effect transistors," *PNAS,* vol. 103, pp. 921-926, 2006.

[12] J. Comley, "LABEL-FREE DETECTION: New biosensors facilitate broader range of drug discovery applications," *Drug Discovery World,* vol. 5, pp. 63-74, 2004.

[13] S. K. Sia and G. M. Whitesides, "Microfluidic devices fabricated in poly(dimethylsiloxane) for biological studies," *Electrophoresis,* vol. 24, pp. 3563-3576, 2003.

[14] T. R. Jones, A. E. Carpenter, D. M. Sabatini, and P. Golland, "Methods for High-Content, High-Throughput Image Based Cell Screening " in *Computer Science and Artificial Intelligence Laboratory (CSAIL)* Cambridge: MIT.

[15] D. J. Beebe, G. A.Mensing, and G. M.Walker, "Physics and applications of microfluidics in biology " *Annu. Rev. Biomed. Eng,* vol. 4, pp. 261–286, 2002.
[16] Y. Xia and G. M. Whitesides, "SOFT LITHOGRAPHY," *Annu. Rev. Mater. Sci.,* vol. 28, pp. 153-184, 1998.
[17] J. M. Shaw, J. D. Gelorme, N. C. LaBianca, W. E. Conley, and S. J. Holmes, "Negative photoresists for optical lithography," *IBM J. Res. Dev,* vol. 41, pp. 81–94, 1997
[18] C. Ionescu-Zanetti, R. M. Shaw, J. Seo, Y.-N. Jan, L. Y. Jan, and L. P. Lee, "Mammalian electrophysiology on a microfluidic platform," *PNAS,* vol. 102, pp. 9112-9117, 2005.
[19] D. A. Chang-Yen, R. K. Eich, and B. K. Gale, " A monolithic PDMS waveguide system fabricated using soft-lithography techniques," *Journal of Light Wave Technology,* vol. 23, pp. 2088-2093, 2005.
[20] K. Haubert, T. Drier, and D. Beebe, "PDMS bonding by means of a portable, low-cost corona system," *Lab on Chip,* vol. 6, pp. 1548-1549, 2006.
[21] A. Tarnok, "A Focus on High-Content Cytometry," *International Society for Advancement of Cytometry,* vol. 73A, pp. 381-383, 2008.
[22] M. ZHAO, W. CHO, F. REGNIER, and D. NOLTE, "Differential phase-contrast BioCD biosensor," *Applied Optics,* vol. 46, pp. 6196-6209, 2007.

BIOGRAPHICAL INFORMATION

Sajal Chirvi was born on 17th May, 1983 in Srinagar, Jammu and Kashmir, India. She completed her Bachelor of Engineering in Biomedical Engineering from Mumbai (Bombay) University, India in May 2004. She served as research trainee engineer at biomedical wing of Bhaba Atomic Research Center, Mumbai, India for one year.

She joined University of Texas at Arlington in spring 2007 to pursue Masters of Science in Biomedical Engineering. Her current research area is integration of microfluidics with optical imaging.